Pramāṇa, Vol. 23, No. 3, September 1984, pp. 351–368. © Printed in India.

Potential double layers in double plasma device

A N SEKAR and Y C SAXENA

Plasma Physics Programme, Physical Research Laboratory, Ahmedabad 380009, India

Abstract. Results of the investigation on the formation of double layers in double plasma device are presented. By appropriate modifications in the biasing conditions, we have been able to obtain both weak ($e\Delta\phi < 10\,KT_e$) and strong double layers ($e\Delta\phi > 10\,kT_e$) in the device. Unlike previous experiments, we have not been limited to potential jumps equal to ionisation potential of the neutral gas. A detailed investigation has been carried out to find out why earlier experiments in similar devices were limited to only weak double layers.

We have also investigated the phenomenon of the so-called psuedo-double layers and have shown that they are potential jumps over the thickness of the order of Debye length and precede plasma expanding with velocity many times the ion-acoustic velocity. They do not represent metastable states of the plasma as suggested by earlier investigators.

Keywords. Plasma double layers; double plasma device; plasma expansion; pseudodouble layers.

1. Introduction

A double layer is a strongly nonlinear plasma process which belongs to the class of BGK solutions of the Vlasov equation (Bernstein *et al* 1957; Montgomery and Joyce 1969). It consists of two thin regions of opposite charge excesses resulting in a large potential drop across the layer (Carlquist 1972). Double-layer investigations have assumed importance due to several reasons. In addition to being a strongly nonlinear plasma process, double layers provide possible mechanism for anomalous plasma resistivity. Particle acceleration in space plasma is important from the point of view of development of high power gas lasers and intense particle beam production (Mohri *et al* 1980) and are closely related to the tandem potential and thermal barriers proposed for the plasma confinement in the magnetic mirror machines.

Experimentally, double layers have been detected in numerous laboratory experiments in different types of laboratory plasmas. These experiments have been reviewed by Sato (1982). Detailed measurements of the structure of these layers can, however, be obtained only in the experiments at low plasma densities. Use of double plasma and triple plasma device (Quon and Wong 1976; Coakley *et al* 1978) has enabled one to resolve the internal structure of double layers mainly because these devices contain a large volume of effectively collision free plasma at such low densities that the Debye length is $\approx$ 1 mm.

In the first experimental observation of double layer in a tenuous plasma, Quon and Wong (1976) reported stable weak double layers in a modified double plasma device. They also observed the double layers to be unstable when $e\phi/kT_e > 4{\cdot}5$. Strong double layers ($e\phi/kT_e > 10$) were achieved in triple plasma device at Iowa University (Coakley *et al* 1978; Coakley and Hershkowitz 1979). These experiments also pointed out problems of the conventional filament discharge plasma mechanism related to the

fact that the discharge introduces energetic primaries into the system in addition to free and trapped particles. Coakley and Hershkowitz (1979) observed that the presence of primaries was a deterrant to achieving strong double layers in their experiment. Special plasma source on low potential side of the double layer was designed for eliminating introduction of primaries into double layer and strong double layers could be achieved only under these conditions. Further, Coakley and Hershkowitz (1979) also reported that stable double layers could be observed in their triple plasma device with source I on high potential side, off. However, the adjustment of density of specially designed source I, appeared to play an important role in deciding the strength of the double layer. In their attempt to duplicate the results of Quon and Wong (1976) in University of Iowa's double plasma device, Coakley and Hershkowitz (1979) were unable to observe double layers; they instead observed, what they termed as pseudo-double layers. They tried to explain these in terms of the plasma possessing two metastable states between which it switched. However, the process was not probed in detail. Leung *et al* (1980) reported further experiments on double layer formation in multiple plasma device. The device was for most of the time operated in double-plasma mode with the source on high potential side, off and stable double layers were obtained. The highest stable potential drop obtained both in the experiments of the Coakley and Hershkowitz (1979) and those of Leung *et al* (1980) were limited to about 14 V in argon plasma. It was thus seen that for some reason the potential drops were limited to about the ionisation potential of the neutral gas in the configurations used in the above mentioned experiment.

These set of experiments created a number of ambiguities. It was not clear whether the stable double layers could be produced in a double plasma device, whether making a triple plasma device with meticulously designed sources was necessary for this purpose, even though one could achieve stable double layers while operating it in double plasma-like mode. Why were the maximum potential drops limited in these devices and what caused the phenomenon of pseudo-double layers in the double plasma device?

In view of these unresolved questions it was decided to investigate the formation of double layers in our double plasma device. In this paper we report the result of our investigations on the generation and properties of the observed stationary double layers. We have also examined in detail the phenomena associated with the pseudo-double layers. With appropriate modification of biasing conditions and control of neutral gas feed, we have also been able to achieve strong double layers with $e\phi/kT_e > 10$ and we have not found any limitation of potential jumps to the ionisation potential in this configuration. This configuration is compared with the configuration used in previous experiments and the reasons for obtaining strong double layers in our case have been analysed. We have not found it necessary to design any special plasma sources for this purpose.

2. Experimental set-up

The experiment was performed in a double plasma machine, consisting of a source and target region as shown in figure 1. The source chamber was made of a cylindrical vessel (30 cm long and 30 cm diameter). Plasma was produced in the source region by electron impact ionisation of neutrals by 60 eV electrons, that were thermionically emitted from 24 numbers (8 cm long) of tungsten filaments. The filaments were mounted in a circular configuration to produce uniform plasma. The anode mesh was left floating for an

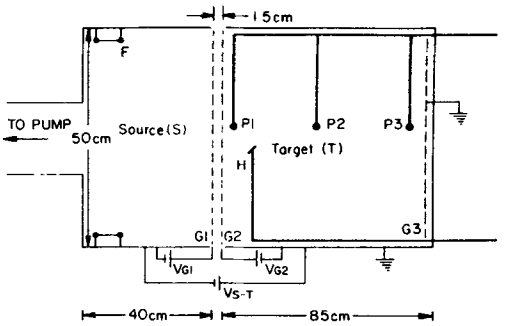

Figure 1. Schematic of the double plasma machine. Drifting electrons are produced by biasing the source chamber negative with respect to the target chamber. F—Filaments, P_1, P_2, P_3—collecting Langmuir probes, H—emissive probe. Grid G1 is biased 0 V with respect to the source, potential of grid G2 is varied from 0–10 V with respect to the target and the end grid G3 is grounded.

effective electrostatic confinement of the primary electrons, and we did not resort to surface magnetic field containment. This assembly was placed in the main vacuum chamber (125 cm long and 50 cm diameter). The plasma in the target region was formed by electron impact ionisation of neutral gas by the ionising electrons flowing from source region to the target region. The target region was separated from the source region by two grids G1 and G2, suitably biased with respect to the two plasmas. The plasma temperature was a few electron volts ($T_e \gg T_i$). The density in the target region ranged between 10^7 and 10^8 cm^{-3}. To generate double layers a potential V_{S-T}(0–300 V) was applied to the source with respect to the grounded target. An end grid G3, which was also grounded, provided the reflected electrons at the high potential region.

3. Diagnostics

The electron temperature, density and the distribution function were obtained from the I-V characteristics of a Langmuir probe. The 1·5 cm diameter movable disc probe was mounted on an insulated shaft. The shaft was placed along the boundary of the wall to minimize its disturbance of the plasma. The output signal from the probe was directly monitored on the oscilloscope, or X–Y recorder.

A hot electron emitting probe was used to measure plasma potential. The floating potential method (Sekar 1982) was deployed. The use of the emissive probe to monitor plasma potential is advantageous in that it responds only to potential energies and not kinetic energies, of the particles. It also provides accurate measurement of plasma potentials especially in the presence of particle beams.

A multi-electrode energy analyser was used to obtain the ion energy distribution and was made of a collector disc and a grid mesh. The outer enclosure was left floating and the grid was biased to collect ions. The I-V characteristics was obtained by varying the collector potential. The distribution was obtained by differentialing the I-V curve.

4. Experimental results and discussion

4.1 *Extended potential structures and moving double layers in an expanding plasma*

4.1*a Results.* Establishment of a double layer in multiple plasma devices seems to critically depend on the pressure of the neutral gas in the device (Leung *et al* 1980). Our initial attempts to produce double layers in a double plasma device were not very successful. At a critical pressure, we instead observed another phenomenon, which could explain the observations of the so-called pseudo-double layers, by Coakley *et al* (1979). We observed (Mattoo *et al* 1980) potential discontinuities resulting from the ionisation of very minute amount of gas that leaks into the system during the scanning of the plasma by the probe. The results were examined in detail and in what follows we present these results.

By biasing the source plasma negative with respect to the target chamber, a large electron current flows from the source to the target chamber. Depending upon the pressure of argon neutral gas, the effect of this current is to lower the plasma potential in the entire target region. The observed plasma potential structures, for fixed bias conditions, at various neutral gas pressures are shown in figure 2.

At low pressures ($\sim 7 \times 10^{-5}$ torr) an extended potential structure, corresponding to a change of $\approx$ 12 volts over 20 cm, is formed with potential minimum adjacent to the grid G2. Of the applied potential between the two chambers, nearly half appears across this extended plasma potential structure, and the rest appears across the sheath formed around end grid G3. The measured electron distribution does not contain any beam component. But it could be represented by two populations of electrons, hot and cold. The I-V characteristics show that the hot component temperatures before ionisation, at P1 and P3, were 10·5 eV and 10 eV respectively. The temperatures after ionisation were about 4·5 and 7·6 eV respectively. The density of the hot component was about $\frac{1}{3}$ of the cold component.

As the cold component is increased, the spatial variation of the plasma potential gets modified. The potential near grid G2 becomes positive and the potential near G3 more negative. At a critical neutral gas pressure, determined by the relative biases on the grids

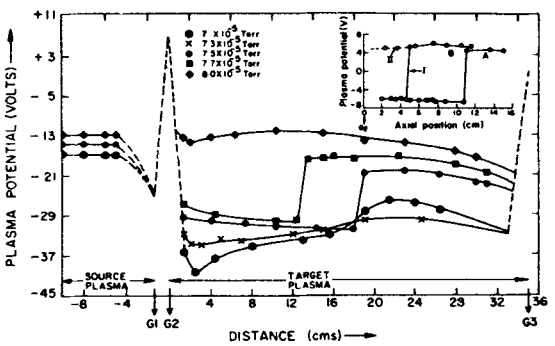

Figure 2. The axial plasma potential profiles in the target chamber at various indicated pressures, obtained by the emissive probe. The inset is a typical potential variation at the critical pressure. Profile A corresponds to when the emissive probe is moved away from the grid G2, and profile B, when the emissive probe is moved towards grid G2. The dashed line (branch II of the profile B) shows that occasionally the entire plasma potential is at high state.

and between the two chambers, the plasma potential undergoes a very sudden transition. The transition occurs over a distance of a Debye length.

Inset of figure 2 illustrates the details of such a sharp potential jump in another typical case.

Profile A is obtained while the emissive probe is moved away from the grid G2. At a certain position in the target chamber, the plasma potential makes a sharp transition from a low-state of -6 V to a high state of 4·4 V in a distance of less than 0·2 cm. At this instance, there occurs a visible increase in the plasma glow, indicating that an enhanced ionisation of neutral gas has occurred. All the collecting Langmuir probes, placed at different positions in the target chamber, showed increase in the plasma density. The maximum increase in the plasma density is registered by the probe placed in the region close to grid G2. At this location, the plasma density increases to about 4 times the ambient value. From the analysis of the characteristics, we do not find any evidence of the presence of an electron beam, with energy less than or equal to the potential jump.

The profile B corresponds to the measurements obtained while the emissive probe is moved from the region of high potential state towards grid G2, immediately after the profile A is obtained. The potential makes a transition from high value to low value at a place which is different from the transition point in profile A. The plasma density falls to the ambient value. This is represented by branch I of the profile B. Occasionally, the plasma potential does not make any such transition and the entire plasma remains at the high potential state (branch II of profile B), and then to realise the initial conditions it becomes necessary to disturb the device controls like the needle valve which maintains the gas flow, or the relative bias between the two chambers.

Two collecting Langmuir probes, P_1 and P_3 placed near G2 and G3 separated by 30 cm, are biased to collect the saturation electron current. Figure 3 shows that the onset of the increase in electron density occurs earlier at the probe near G2 than grid G3, when a transition in the plasma potential is affected by moving the emissive probe away from the grid G2. This indicates that the potential jump is accompanied by a moving plasma. The plasma moves in the direction away from grid G2 and towards G3 at a velocity $\approx 10^4$ m sec^{-1}. At a given position in the target region the onset of the increase in the electron density occurs simultaneously with the increase in the plasma potential at that position. Also, the velocity measured by two emissive probes is the same as that measured by two collecting probes collecting electrons. The velocity direction remains the same even when the transition in the plasma potential is affected by moving the emissive probe towards the grid G2. Thus the plasma potential jumps shown in figure 2 are not stationary structures.

To locate the source of the moving plasma, the variation of the plasma potential near the grid G2 was noted as the neutral gas pressure was varied. This is shown in figure 4. It shows that as the pressure of the neutral gas is changed from $1{\cdot}30 \times 10^{-4}$ to $1{\cdot}35 \times 10^{-4}$ torr, the plasma potential makes an abrupt jump from $-13{\cdot}2$ to 6 V. The implication of this result is that a sharp transition of the plasma potential can be effected by a minute amount of the neutral gas and this can occur only when the device is tuned to a critical pressure. The value of the critical pressure depends upon the relative bias between the chambers. At larger bias voltages, the critical pressure is low. It thus appears that during the movement of the probe a very minute amount of gas leaks into the device and ionisation of this gas on reaching the grid G2 leads to the source of moving plasma.

Another feature of the potential jumps is that the high-state plasma potential is

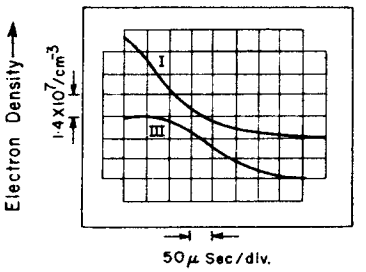

Figure 3. Oscilloscope trace of time profile of the saturation electron currents obtained by collecting Langmuir probe P_1 and P_3. Figure shows that the arrival of the plasma blob at P_3 is delayed by ≈ 30 μsec with respect to the same at P_1.

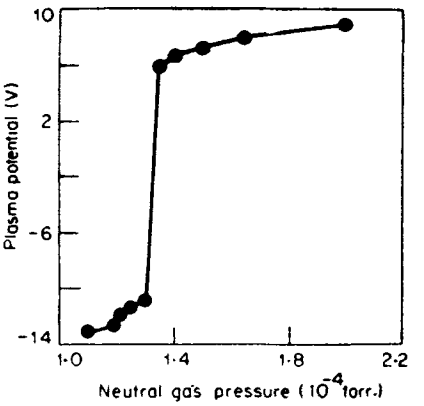

Figure 4. The plasma potential near G2 is plotted for various neutral gas pressures. The device control settings are G1 = 0 V and G2 = 10 V, G3 is grounded and $V_{S-T} = -8{\cdot}3$ V. Note the sharp transition in the plasma potential between 1·3 and 1·35 $\times 10^{-4}$ torr.

related to the potential of the grid G2. The value of the high-state potential increases with the bias voltage of the grid G2.

At 8×10^{-5} torr, the entire target plasma attains uniform potential. The difference between the source and target plasma potentials becomes very small. The applied bias voltage appears across the space charge sheaths of G3 and the end plate of the source chamber. Any further increase in neutral gas pressure, makes very little change in the spatial variation of the plasma potential profile in the source and target chambers.

4.1*b Discussion.* Below a critical pressure, the electron current extracted from the source establishes an extended potential structure in the target plasma. This has a potential structure continuously varying in space and does not constitute plasma double layer. What seems to sustain the extended potential structure in our case is the variation in the electron temperature of the hot component of the electron distribution.

If a potential double layer is to exist, the ion density in the low potential region must be less than the electron density. This explains why a critical adjustment of pressure of the neutral gas is required to produce a double layer.

We have demonstrated that the observed potential jumps are accompanied by a moving plasma. Figure 4 suggests that the origin of the plasma blob may be in the enhanced ionisation of a very minute amount of the gas that leaks into the system by the movement of the probe. That the plasma blob is formed in the region adjacent to the grid G2, is evidenced from velocity measurements. This also rules out the explanation of anode sheath. The measured velocity of the leading edge of the created plasma is 5 $(kT_e/M_i)^{1/2}$.

The observed high velocity is due to plasma expansion resulting from the thermal pressure in the plasma. The initial response of the plasma to the thermal pressure is that the warm electrons will separate out to form a region of electron charge concentrated near the density discontinuity. The electrons on the average will separate from the ions by a distance of a Debye length, so that at the boundary a double layer (thickness of the

order of Debye length) will be formed. The electrons cannot go further due to the electric field and ions which immediately follow will be accelerated. This would mean that the leading edge of the ions in the double layer will be moving at a velocity faster than the ion acoustic speed. An explanation of the observed potential jumps and the large velocities can be correlated with electron temperature. This is presented below in the model based on the adiabatic expansion of plasma and hence acceleration of ions by the ambipolar fields.

Following Hendel and Reboul (1962), a thermodynamic collisionless model leads to an adiabatic transfer of energy from electrons to ions. The conditions necessary for such a mechanism to exist are (i) the existence, in the discharge, of a constant source of electrons with adequate energies. (ii) Concentration of charged particles at the front of the expanding plasma cloud sufficient enough for creating a space charge cloud capable of accelerating ions. As both the conditions are satisfied in our experiment, the above model is applicable. The electrons gain relatively high energy from the applied field, while the energy transferred to ions from the external field, and electron ion collisions are negligible. Randomization of electron velocity is obtained in a few microseconds. High velocity electrons attempt to escape isotropically from the plasma, but are restrained by the electric field of the ions to a distance of a Debye length.

The space charge set up by the electrons accelerates a spherical ion piston radially. Since we are considering a one-dimensional case, we can treat this as a plasma expansion in a single direction. The energy needed for the ions is supplied by the initial energy content of electron gas. During the short period of ion acceleration by space charge, only a negligible amount of heat can be delivered to ions by collisions with electrons due to a limited transfer of momentum in such a collision. So energy transfer is adiabatic.

The work done by the electron gas at T_1 and pressure P on the ion piston during the expansion from volume v_1 to v_2 is given by

$$W = \int_{v_1}^{v_2} P \, \mathrm{d}v. \tag{1}$$

This work sets up a space charge field accelerating ions towards electrons and simultaneous decelerations of electrons.

Using Poisson's adiabatic law

$$Pv^{\gamma} = C, \tag{2}$$

with $\gamma = 5/3$, and the general gas law

$$Pv = nkT \tag{3}$$

From (2) and (3) we get

$$v^{-2/3} = nkT/C. \tag{4}$$

Differentiating (4) we get

$$-2/3\, v^{-5/3} \mathrm{d}v = nk\mathrm{d}T/C. \tag{5}$$

From (2)

$$-P\mathrm{d}v = 3/2\, nk\mathrm{d}T. \tag{6}$$

Substituting (5) in (1) we get

$$W = \frac{1}{2} nMV^2 = -\frac{3}{2}\int_{T_1}^{T_2} nk\mathrm{d}T$$

which gives

$$V = (3k(T_1 - T_2)/M)^{1/2} \tag{7}$$

Equation (7) is the drift velocity acquired by the ions.

Thus when ions and electrons finally drift at the same velocity, electron energy is transferred to ions, the final ion energy being almost equal to the initial electron energy. Momentum is conserved since the centre of mass of the expanding plasma is at rest.

From the I-V characteristics, at the probe P_1, we have electron temperatures before and after ionisation to be 10·5 eV and 4·5 eV respectively. From equation (7)

$$V_{\text{ion}} \approx 4C_s.$$

This is quite in agreement with the experimental result of $5C_s$.

Hence an adiabatic thermodynamic model agrees quite well in the case of expanding plasmas, where ions are accelerated to sufficiently large velocities.

Computer simulations, that do not use Boltzman distribution for the electrons and charge neutrality have obtained a maximum velocity of the leading edge to be $5C_s$, which is the same as our observed result. What is important is not that the measured velocity can be explained by the expansion of a plasma blob. The important point to note is that the expansion of the plasma is accompanied by a double layer at the leading edge of the plasma blob and its thickness is one Debye length. Thus it seems likely that potential jumps correspond to the moving double layers formed as a consequence of the expansion of the plasma, created due to the ionisation of the leaked gas adjacent to the grid G2.

We have observed that potential jumps occur only when the device is tuned to a critical pressure. Having identified the cause of these jumps in the formation of a plasma blob, it means that enhanced ionisation of the gas that leaks into the system during the movement of the probe occurs only when the neutral pressure is at a critical value. However as the ionisation mean-free path of ionising electrons in the target plasma decreases very negligibly when the gas pressure changes by a very small fraction of the ambient pressure, an explanation is required for the cause of the enhanced ionisation at the critical pressure. We explain it as follows:

The energetic electrons in the target chamber ionise a fraction of the leaked gas at the high potential end, producing ions and low energy electrons. The low energy electrons are trapped between the sheath around the grid G3 and the potential minimum located near the grid G2. The ions in the high potential side are accelerated towards the potential minima and reflected at the sheath of the grid G2.

Thus the potential well near the grid G2 becomes shallower. This in turn allows more electrons to be extracted from the source and hence more ionisation of the gas. The critical effect may arise due to the fact that, at this pressure, the plasma region adjacent to the grid G2 attains momentarily an accelerating potential of the order of ionisation potential of the gas with respect to the source. Since the ionisation cross-section of the gas increases rapidly at the ionisation potential, the accelerated electrons extracted from the source leads to an enhanced ionisation of the gas adjacent to the grid G2. This creates a plasma blob in which a potential double layer develops at the leading edge at a later stage.

An interesting feature of these results is the acceleration of ions in the direction of electron drift. Such observations have been made in the space observations of

Ghielmetti *et al* (1979) and also in the computer simulation of Singh (1982) in moving double layers.

Our observations of potential jumps may be similar to those obtained by Coakley and Hershkowitz (1979). However, we do not attribute these potential jumps to the existence of two metastable states in the plasma. We wish to state that invoking the existence of metastable state would require far more complicated plasma processes than the simple explanation offered here.

4.2 *Weak double layers*

The experiment was performed in a double plasma machine shown in figure 1. The grid G1 was biased with respect to the source and grid G2 was biased with respect to the target. The operating pressures ranged from 4×10^{-5} torr to 3×10^{-4} torr. The plasma parameters were as mentioned earlier. Operating at the normal mode grids G1 and G2 were biased at 0 eV. The target chamber and the end grid G3 were both grounded, keeping the source chamber floating. The potential of the source plasma was varied by applying bias voltage with respect to the target chamber. The axial potential profiles at a fixed relative bias, but different neutral gas pressures, are shown in figure 5. The potential drop across the double layer was about 8 to 10 V, *i.e.* $e\Delta\phi \simeq 4$–$5\ kT_e$. The electron energy distribution in the presence of a double layer in one of the cases (profile c in figure 5) is shown in figure 6. As a result of electron flow, which was maintained by a drift velocity $1{\cdot}3\ V_{th}$ (V_{th} = electron thermal velocity), a negative potential well was formed near grid G2. There was a beam component near grid G2 which modified to a drifting distribution function at the trough of the potential. Accelerated electrons were observed at the high potential side of the double layer. These components were observed to thermalise in a distance of about 10 cm ($50\ \lambda_D$) from the high potential side of the double layer. The spatial extent of the double layer was about 12 cm ($60\ \lambda_D$). The

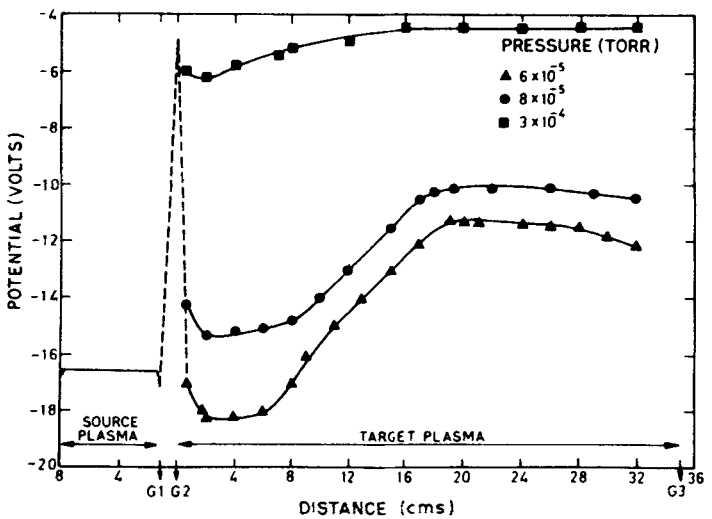

Figure 5. Axial potential profiles in the target chamber at different pressures and a fixed relative bias. Profile A (■) corresponds to the shallow potential structure and profile C (Δ) corresponds to the double-layer potential profile.

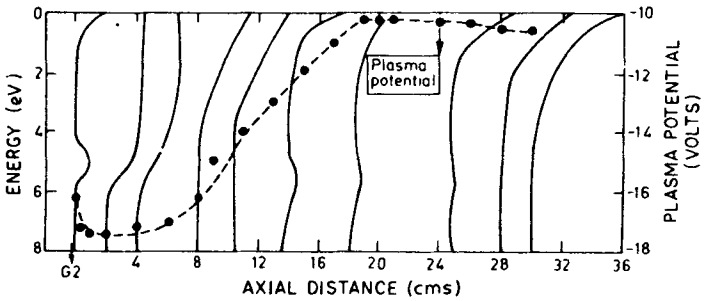

Figure 6. Electron energy distribution functions at various space points corresponding to profile C of figure 5. The potential profile is represented by dashed line. Drifting electron distribution is present on the low potential side and accelerated component which thermalises in a distance of about 10 cm is present on the high potential side.

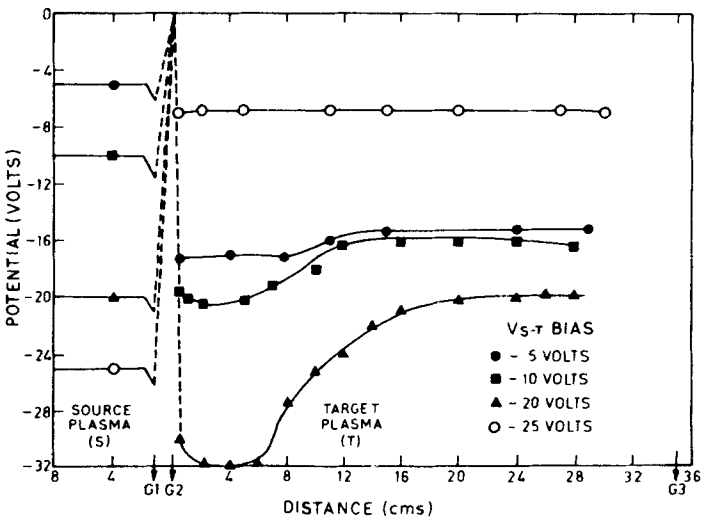

Figure 7. Axial potential profiles in the target chamber at different relative bias voltages, keeping the pressure constant. Profile B(o) corresponds to the shallow potential structure, at a large relative bias.

range of pressures at which the double layer could be formed was between 4×10^{-5} and 8×10^{-5} torr. The potential profiles for a fixed gas pressure at various relative biases are shown in figure 7.

We observed a criticality in both neutral gas pressures and relative biases in forming the double layers. This can be clearly viewed from the shallow potential structures of A in figure 5 and B in figure 7. Ionisation of neutral gas played a crucial role in deciding the criticality in both the cases. At low neutral gas pressures there was a large potential minimum formed near G2 as a result of electron flow from the source. The potential then rose towards G3 and under suitable conditions of bias voltages transformed into a double layer. As neutral gas pressure was increased it led to a larger ionisation and the newly produced ions reduced the space charge of the electrons at the potential minimum. A further increase of pressure-enhanced ionisation and hence a further

reduction in the potential drop. The potential change in the entire chamber was about 1 to 2 V. Similar results were observed at large relative bias voltages when the beam electrons were energized sufficiently to ionize the neutral gas in the target chamber. These observations indicate the crucial role of ionisation of neutral gas as reported in the earlier experiments (Leung *et al* 1980; Coakley and Hershkowitz 1979) in the formation of double layers.

The present results show that a relative electron drift velocity $V_d = 1{\cdot}3\ V_{th}$ was necessary to form a double layer, which also corresponds to the results of Quon and Wong (1976). Plasma in the target chamber was produced by ionisation of neutral gas, by the high energy ionising electrons, which drifted into the target chamber. As a result we have in our distribution function near G2, a low energy electron component and a higher energy beam that has been accelerated by a suitable relative bias. The distribution function at the trough of the potential is modified to a drifting distribution. A plausible explanation for this could be, that the beam is slightly decelerated by the fall in the potential; further the low frequency instabilities produced can redistribute its energy to the low energy components. The resultant drifting distribution leads to the formation of a double layer. The presence of the electron current which is maintained by a constant flow of electrons creates a potential minimum where the ions get trapped. As the potential rises the electrons are accelerated which can be seen from the distribution function. As we do not provide a separate source of trapped electrons like the triple plasma device of Coakley and Hershkowitz (1979), the presence of the low energy electrons is due to the ionization of neutral gas and thermalisation of the accelerated particles. The hot electrons that travel towards the double layer are reflected at the layer while those moving away are reflected at the end grid G3 thereby maintaining the necessary trapped population of electrons at the high potential region. Ions accelerated from the high potential region get reflected at G2 and together with the ions produced near the grid G2 provide the necessary reflected particles at the low potential side.

The thermalisation length of the beam electrons which is about 10 cm ($50\,\lambda_D$) is comparable to those observed by Quon and Wong (1976). From the theoretical calculation for beam plasma interaction, we obtained a length of about 15 cm ($75\,\lambda_D$) for the thermalisation of the beam electrons. This corroborates our experimental observations.

From the computer simulations of the Joyce and Hubbard it was observed that the spatial extent of the double layer was $L_{dl} \approx 6(e\phi/T_e)^{1/2}$. This agrees very well with our results where $L_{dl} = 5$ to $6(e\phi/T_e)^{1/2}$. This is also in agreement with the theoretical investigations (Knorr and Goertz 1974) where a lower limit for the width of the double layer of $L_{dl} = 3(e\phi/T_e)^{1/2}$, was obtained.

As surface magnetic fields were not employed, the primary ionizing electrons drifted into the target chamber overcoming the potential barrier at G2. These electrons may produce plasma in the double layer region and thus limit the potential drop, to smaller voltages. The currents involved in this configuration are also limited to small values and this may also limit the amplitude of the potential drop. This is discussed in detail in the next section.

4.3 *Strong double layers*

With the biasing configuration as shown in figure 1, which is similar to that used by Quon and Wong (1976), Coakley *et al* (1978) and Leung *et al* (1980), we were able to

obtain only weak double layers in a critical range of parameters. But on modification of the biasing system we could obtain strong stable double layers with $e\Delta\phi \approx 20\,T_e$. The modified biasing arrangement is shown in figure 8. In the earlier configuration (configuration I), the two grids were biased positive with respect to the adjacent chambers. In the modified configuration (configuration II) both the grids were biased positive with respect to the source chamber which was given bias relative to target chamber. The gas feed was also shifted from target chamber side to source chamber and pumping was done from the target chamber side.

The axial potential profiles obtained in configuration II are shown in figures 9 to 11 for different relative bias voltages varying from 0 to 300 volts. The potential drop increase with relative bias is observed. The stronger double layers are produced closer to grid G2. At large relative biases ($\gtrsim$200 V) a knee is observed in the potential profile

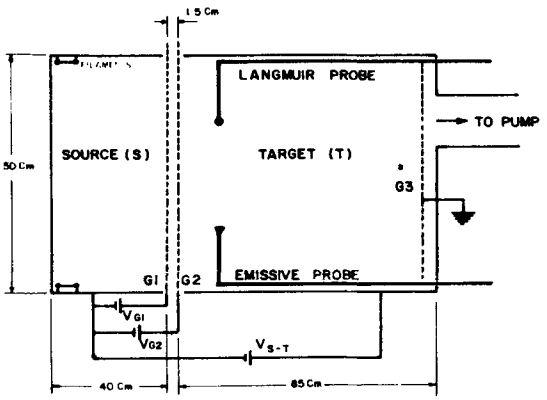

Figure 8. Configuration II, modified to obtain strong double layers. Grids G1 and G2 have been biased with respect to source, and the pumping unit is on the target region with gas feed in source region. Drifting electrons are injected from the source into the target chamber by the relative bias. G1 and G2 are normally biased to 0 V.

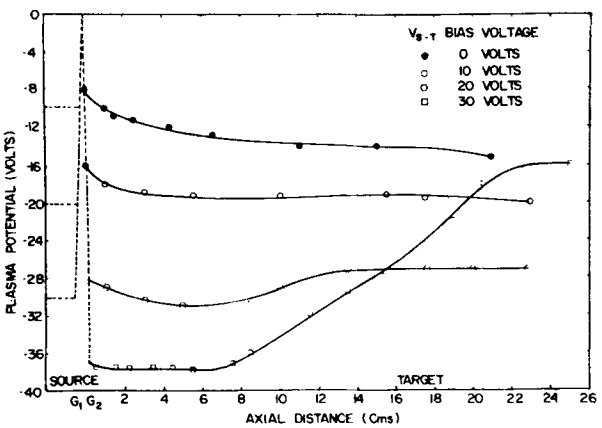

Figure 9. Axial plasma potential profile in the target chamber, at different relative bias voltages varied from 0–30 V.

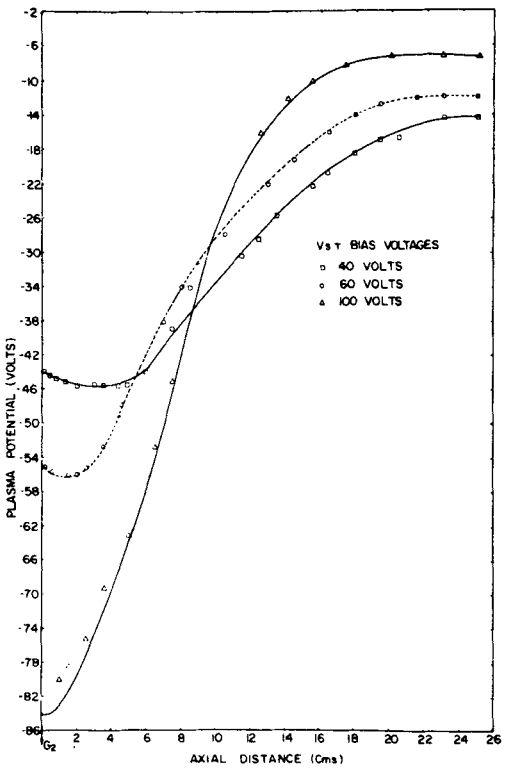

Figure 10. Axial plasma potential profiles in the target chamber, at different relative bias voltages varied from 40–100 V.

(figure 11) and at larger biases (250–350 V) a negative potential dip on the low potential side of the double layer.

The amplitude of the double layer also depends upon the bias on grid G2. The potential profiles for various G2 bias voltages are shown in figure 12. As G2 is made more positive, the potential drop is reduced. A similar behaviour is also observed in the case of G1 bias voltage.

In this configuration, we were able to obtain the double layers over a wider range of neutral pressure compared to configuration I. Figure 13 shows the axial potential profiles for different neutral pressures. The potential amplitude decreases with increasing pressure.

The electron distribution function for one typical case of the strong double layer is shown in figure 14. In the proximity of grid G2, there is a free electron distribution function which undergoes a small deceleration due to negative potential well, and at the transition region, we observe accelerated particles, which thermalise in a distance of about 6 to 8 cm from the high potential region.

The electron and ion currents were monitored in the absence of (figure 15), presence of weak (figure 16) and strong (figure 17) double layers. We find that there is a depletion in the currents in the region of potential change. The spatial separation of the depletion is an indication of charge separation giving rise to double layers. The current depletion increases in the case of strong double layers.

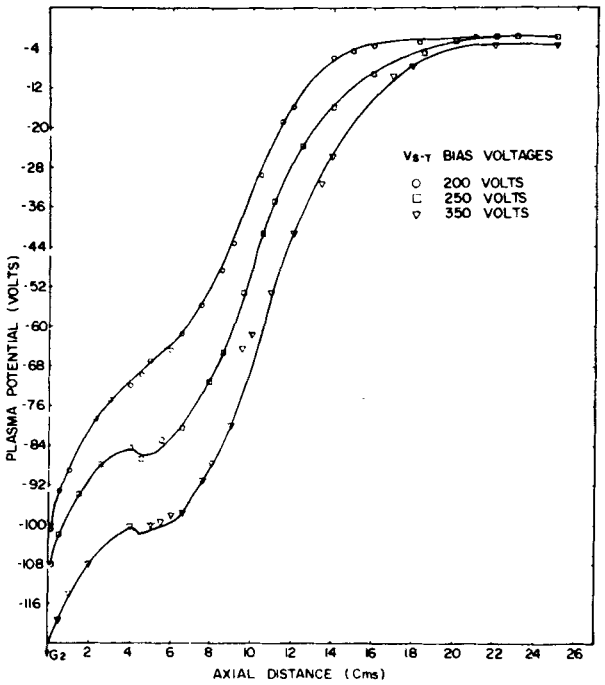

Figure 11. Axial plasma potential profiles in the target chamber, at different relative bias voltages varied from 200–350 volts. Note the presence of a knee-like structure and a clear potential dip after the sheath-like structure. This closely resembles the multiple double layers.

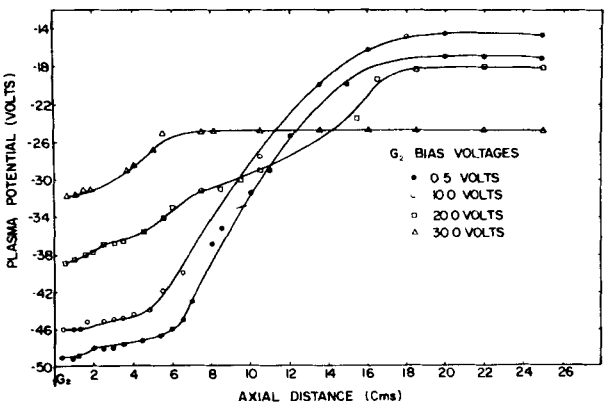

Figure 12. Axial plasma potential profiles in the target chamber at different G2 bias voltages keeping the relative bias voltages and neutral pressure constant.

4.3*a Discussion.* We have thus been able to form strong double layers which are not limited to the ionisation potential of neutral gas, nor to the electron temperature but depend more on the current injected into the system. We attribute this to the fact that by modifying the biasing arrangement in configuration II we can extract larger electron current from the source and hence obtain larger potential jumps. To verify this we

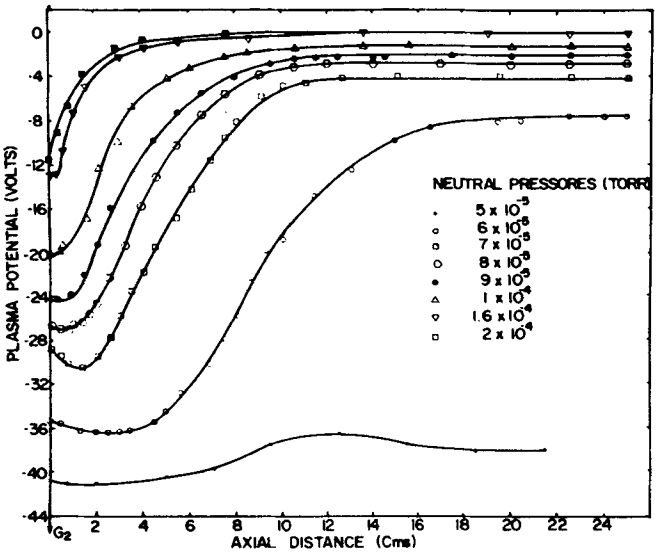

Figure 13. Axial plasma potential profiles in the target chamber at different neutral pressures, keeping the relative bias voltage and grid bias voltages constant.

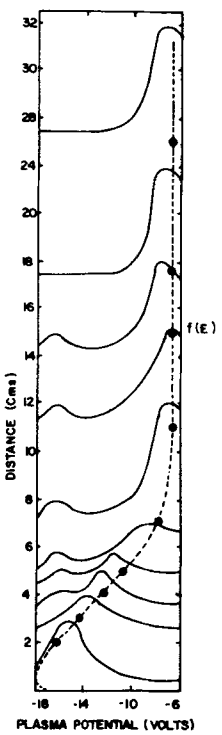

Figure 14. Electron distribution function obtained in the presence of a double layer. Potential profile is shown by dotted lines. The plots are obtained at different axial distances in the target region after forming a double layer.

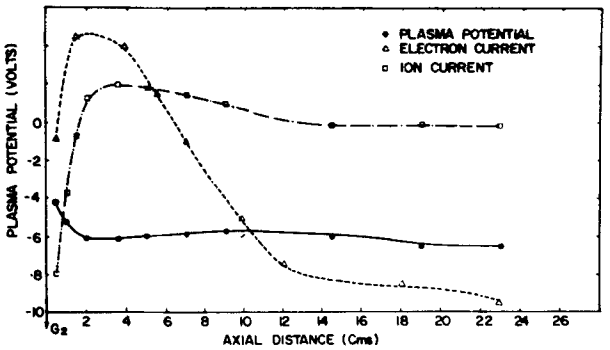

Figure 15. Plots of plasma potential, electron current and ion current in the target chamber, in the absence of a double layer. Electron currents are in mA, and ion currents are in μA.

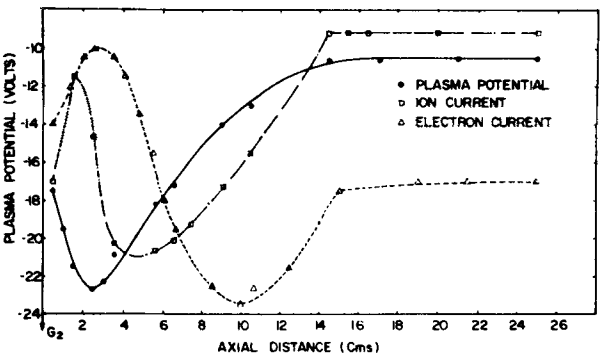

Figure 16. Plot of the plasma potential (thick line), electron current (dashed lines), ion current (dot and dashed lines), in the target chamber when a weak double layer was formed. The electron and ion currents are in mA and μA respectively.

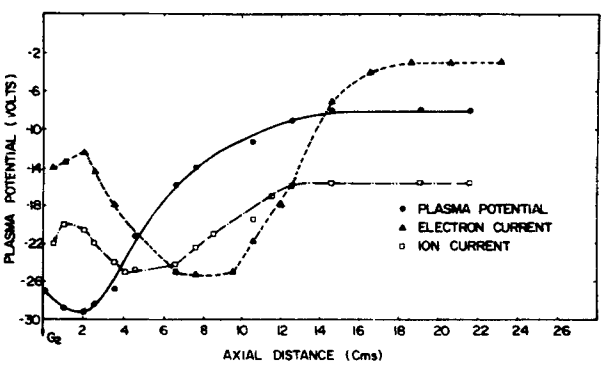

Figure 17. Plot of plasma potential (thick line), electron current (dashed lines) and ion current (dot and dashed lines), in the target chamber in the presence of a strong double layer. The electron and ion currents are in mA and μA respectively.

monitored the electron beam current in the two configurations. The probe biased sufficiently negative to collect only high energy electrons, but repeal low energy electrons was placed close to grid G2. The beam current was thus monitored at various bias voltages in the two configurations (figure 18). In configuration I, the current initially increased, but at higher relative biases, decreased with increasing bias. On the contrary, in configuration II, we found that the current increased with relative bias before saturating at larger bias potentials. In configuration I weak double layers were formed only in the narrow range of current rise. Beyond this range the entire plasma attained a uniform state. But in configuration II, the double layers were formed over a wide range of bias potential. It is thus clear that the magnitude of the double layer depends on the current injected into the target region.

The observed reduction in double layer amplitude with increasing neutral gas pressures is well understood. The ionisation increases as neutral gas pressure increases and this generates more ions. The increased ion density neutralises the excess negative charge on low potential side resulting in reduction of the potential jump amplitude. The reduction in the amplitude of potential jump with increasing G2 bias is attributed to the fact that with increasing bias G2 collects more current resulting in reduction of current injected in target section and hence reduction in potential jump amplitude.

A simple circuit analysis of the configurations I and II show that net current flowing into the target region in configuration I is always less than the total current flowing from the source by an amount equal to the current flowing in grid G2, whereas in configuration II, the total current originating in the source flows into the target region. In configuration I, it is observed that the net current flowing into the target region decreases as the source target bias voltage (V_{S-T}) is increased. This could be attributed to the increase in the current flowing to grid G2. This has been established by monitoring the electron current in G2 separately in each of the two cases. It is found that in configuration I, the current through G2 increased with V_{S-T}, whereas in configuration II, the current initially reduced slightly and then remained nearly constant with increasing V_{S-T}.

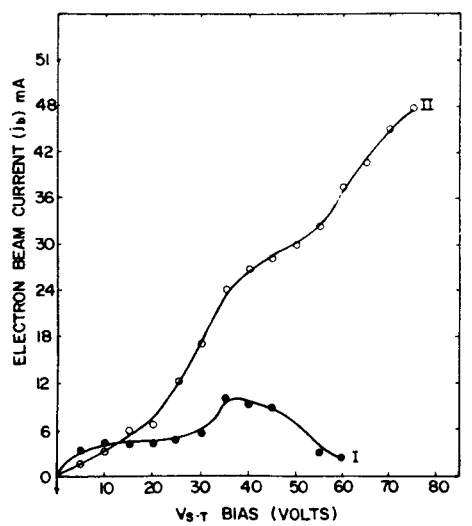

Figure 18. Plot of the beam electron current in the two configurations I and II *vs* V_{S-T}. The current was monitored at a distance of 2 cm from the grid G2 in the target region, with a Langmuir probe biased to collect energetic electrons.

Our results demonstrate that it is possible to produce strong double layers, in a double plasma machine. The external circuit plays a crucial role in this and larger currents flowing into the target regions are essential to produce double layer. The ionisation potential of neutral gas has not been found to be a limiting factor in configuration II.

5. Conclusions

We have described experiments involving the formation of double layers in double plasma device. Our results lead us to the following conclusions: (a) Pseudo-double layers, observed in this device, are due to the expansion of high density plasma blob into the lower density plasma and are not associated with the plasma possessing metastable states. They are observed at critical parameter settings. (b) The strength of the double layers formed in the double plasma machine depends upon the strength of electron current flowing from the source to target region, which in turn depends upon the external circuit conditions. Both weak and strong double layers can be formed. (c) The potential jumps in the double layers are not limited to the ionisation potential of the neutral gas. We have demonstrated that using biasing arrangements corresponding to configuraion II, strong double layers, with potential jumps much larger than the ionisation potential of the gas, could be obtained.

References

Bernstein I B, Greene J M and Kruskal M D 1957 *Phys. Rev.* **108** 546
Carlquist P 1972 *Cosmic Electrodyn.* 3 377
Coakley P Hershkowitz N, Hubbard R and Joyce G 1978 *Phys. Rev. Lett.* **40** 230
Coakley P and Hershkowitz N 1979 *Phys. Fluids* **22** 1171
Ghielmetti A G, Sharp R D, Shelly E G and Johnson R G 1979 *J. Geophys. Res.* **84** 5781
Hendel H W and Reboul T T 1962 *Phys. Fluids* **5** 360
Knorr G and Goertz C 1974 *Astrophys. Space Sci.* **31** 209
Leung P, Wong A Y and Quon B H 1980 *Phys. Fluids* **23** 992
Mattoo S K, Saxena Y C and Sekar A N 1980 *Pramana* **15** 525
Mohri A, Narihara K, Tomita Y, Tsuzuki T, Kabeya Z, Akaishi K and Miyahara A 1980 *Jpn J. Appl. Phys.* **19** L174
Montgomery D and Joyce G 1969 *J. Plasma Phys.* 3 1
Quon B H and Wong A Y 1976 *Phys. Rev. Lett.* **37** 1393
Sato N 1982 *Symp. on Plasma Double Layers*, Riso National Laboratory, 116
Sekar A N 1982 *Proc. Indian Natl. Sci. Acad* **A48** 256
Singh N 1982 *J. Geophys. Res.* **87** 3561